JACC: CARDIOVASCULAR IMAGING
VOL. 9, NO. 9, 2016

ISSN 1936-878X/$36.00
PUBLISHED BY ELSEVIER
http://dx.doi.org/10.1016/j.jcmg.2016.01.034

Targeted Near-Infrared Fluorescence Imaging of Atherosclerosis

Clinical and Intracoronary Evaluation of Indocyanine Green

Johan W. Verjans, MD, PhD,[a,b] Eric A. Osborn, MD, PhD,[a,c] Giovanni J. Ughi, PhD,[d] Marcella A. Calfon Press, MD, PhD,[a] Ehsan Hamidi, PhD,[d] Antonios P. Antoniadis, MD, PhD,[e] Michail I. Papafaklis, MD, PhD,[e] Mark F. Conrad, MD,[f] Peter Libby, MD,[e] Peter H. Stone, MD,[e] Richard P. Cambria, MD,[f] Guillermo J. Tearney, MD, PhD,[d,g] Farouc A. Jaffer, MD, PhD[a,c,d]

ABSTRACT

OBJECTIVES This study sought to determine whether indocyanine green (ICG)–enhanced near-infrared fluorescence (NIRF) imaging can illuminate high-risk histologic plaque features of human carotid atherosclerosis, and in coronary atheroma of living swine, using intravascular NIRF-optical coherence tomography (OCT) imaging.

BACKGROUND New translatable imaging approaches are needed to identify high-risk biological signatures of atheroma. ICG is a U.S. Food and Drug Administration–approved NIRF imaging agent that experimentally targets plaque macrophages and lipid in areas of enhanced endothelial permeability. However, it is unknown whether ICG can target atheroma in patients.

METHODS Eight patients were enrolled in the BRIGHT-CEA (Indocyanine Green Fluorescence Uptake in Human Carotid Artery Plaque) trial. Five patients were injected intravenously with ICG 99 ± 25 min before clinically indicated carotid endarterectomy. Three saline-injected endarterectomy patients served as control subjects. Excised plaques underwent analysis by intravascular NIRF-OCT, reflectance imaging, microscopy, and histopathology. Next, following ICG intravenous injection, in vivo intracoronary NIRF-OCT and intravascular ultrasound imaged 3 atheroma-bearing coronary arteries of a diabetic, cholesterol-fed swine.

RESULTS ICG was well tolerated; no adverse clinical events occurred up to 30 days post-injection. Multimodal NIRF imaging including intravascular NIRF-OCT revealed that ICG accumulated in all endarterectomy specimens. Plaques from saline-injected control patients exhibited minimal NIRF signal. In the swine experiment, intracoronary NIRF-OCT identified ICG uptake in all intravascular ultrasound–identified plaques in vivo. On detailed microscopic evaluation, ICG localized to plaque areas exhibiting impaired endothelial integrity, including disrupted fibrous caps, and within areas of neovascularization. Within human plaque areas of endothelial abnormality, ICG was spatially related to localized zones of plaque macrophages and lipid, and, notably, intraplaque hemorrhage.

CONCLUSIONS This study demonstrates that ICG targets human plaques exhibiting endothelial abnormalities and provides new insights into its targeting mechanisms in clinical and experimental atheroma. Intracoronary NIRF-OCT of ICG may offer a novel, clinically translatable approach to image pathobiological aspects of coronary atherosclerosis. (Indocyanine Green Fluorescence Uptake in Human Carotid Artery Plaque [BRIGHT-CEA]; NCT01873716)
(J Am Coll Cardiol Img 2016;9:1087–95) © 2016 by the American College of Cardiology Foundation.

From the [a]Cardiovascular Research Center, Division of Cardiology, Massachusetts General Hospital, Boston, Massachusetts; [b]Department of Cardiology, University Medical Center Utrecht, Utrecht, the Netherlands; [c]Cardiology Division, Beth Israel Deaconess Medical Center, Harvard Medical School, Boston, Massachusetts; [d]Wellman Center for Photomedicine, Massachusetts General Hospital, Harvard Medical School, Boston, Massachusetts; [e]Cardiovascular Division, Brigham and Women's Hospital, Harvard Medical School, Boston, Massachusetts; [f]Division of Vascular Surgery, Massachusetts General Hospital, Harvard Medical School, Boston, Massachusetts; and the [g]Department of Pathology, Massachusetts General Hospital, Harvard Medical School, Boston, Massachusetts. Dr. Verjans has received Rubicon grant 825.12.013 from the Netherlands Organization for Scientific Research. Dr. Osborn has received Harvard Catalyst National Institutes of Health grant KL2 TR001100. Drs. Antoniadis and Papafaklis have received George D. Behrakis Cardiovascular Research Fellowships. Dr. Libby has received sponsored research grants from General Electric, GlaxoSmithKline, and Novartis; and has received National Institutes of

ABBREVIATIONS AND ACRONYMS

CEA = carotid endarterectomy

ICG = indocyanine green

NIRF = near-infrared fluorescence

OCT = optical coherence tomography

The identification of high-risk atherosclerotic plaques likely to cause myocardial infarction or stroke requires new approaches. In conjunction with near-infrared fluorescence (NIRF) molecular imaging agents, intravascular NIRF imaging is a promising new approach to image biological aspects of high-risk atheroma in coronary artery–sized vessels (1,2). In addition, the combination of NIRF molecular imaging with optical coherence tomography (OCT), a clinical high-resolution structural imaging approach, offers both molecular and morphological information, as well as quantitative NIRF imaging (3). Yet a major barrier to the clinical translation of NIRF imaging remains the lack of clinically approved NIRF imaging agents that specifically target high-risk features of atherosclerosis.

SEE PAGE 1096

Indocyanine green (ICG) remains an intriguing candidate agent to enable targeted NIRF imaging of atherosclerosis. ICG, an amphiphilic near-infrared fluorophore, has received approval by the U.S. Food and Drug Administration as a perfusion agent for cardiac output measurements, liver function tests, and ophthalmic angiography, and it has an excellent safety profile (4). Our recent experimental study demonstrated the following: 1) cultured macrophages and foam cells can internalize ICG, putatively by direct binding to albumin or low-density lipoprotein; 2) in atherosclerotic rabbits, ICG targeted plaque lipid and macrophages, and deposited in areas of enhanced endothelial permeability delineated by Evans Blue stain; and 3) ICG enabled rapid intravascular NIRF imaging of rabbit atherosclerosis in vivo (5), a finding subsequently confirmed by Lee et al. (6). Yet given the differences in the complexity and size of human atherosclerosis compared with that of experimental atherosclerosis, it remains unclear whether ICG can target atherosclerosis in living patients and, if so, which aspects of human atherosclerosis. In addition, the ability of ICG to provide sufficient targeting sensitivity to enable NIRF imaging of atherosclerosis in coronary arteries in vivo requires further investigation.

To advance the potential of intracoronary NIRF molecular imaging, here we report the following: 1) a first-in-human study of ICG targeting to atheroma in vivo prior to carotid endarterectomy (CEA); and 2) a first in vivo intracoronary NIRF-OCT imaging study of ICG targeting of coronary atheroma in swine.

METHODS

HUMAN STUDY OF ICG PLAQUE TARGETING. The BRIGHT-CEA (Indocyanine Green Fluorescence Uptake in Human Carotid Artery Plaque) study was approved by the institutional review board of the Partners Human Research Committee (ICG patients, approval #2012P000895; control patients for discarded human samples, approval #2013P002190). Written informed consent was obtained from all patients who received intravenous ICG. Inclusion criteria were scheduled elective CEA, age older than 18 years, and a signed informed consent. Exclusion criteria were hemodynamic instability, pregnancy or lactation, any history of iodide/seafood allergy, renal failure, liver failure, bleeding diathesis, or stroke in the preceding 3 months. Five patients scheduled for clinically indicated CEA (significant stenosis and/or signs of cerebral ischemia) were administered ICG in this pilot study, and 3 patient plaques without ICG injection served as control subjects (who received saline).

ICG, possessing a blood half-life of ~3 min in subjects with normal liver function, was injected intravenously (0.25 mg/kg, up to 25 mg maximum dose over 1 min; Akorn Pharmaceuticals, Lake Forest, Illinois; outpatient ophthalmic angiography routinely uses an identical ICG dose). Patients were then transported to the operating room for CEA. Control plaques were collected from the operating room immediately after CEA and transported in cold saline to the imaging facility within 15 to 30 min. All 8 patient samples were analyzed.

Health grant R01 HL080472. Dr. Stone has received a George D. Behrakis Cardiovascular Research Fellowship. Dr. Tearney has the right to receive licensing royalties from Terumo, Canon, and MIT; has received sponsored research from Canon Inc. and Ardea Biosciences; has received National Institutes of Health grant R01 HL093717 (for development of imaging console and catheter); and has received catheter components from Terumo. Dr. Jaffer has the right to receive licensing royalties from Canon; received sponsored research grants from Kowa, Siemens, and Canon; has received National Institutes of Health grants R01 HL108229 and R01 HL122388-01A1; has received American Heart Association grant 13GRNT17060040; has received Massachusetts General Hospital SPARK award and Executive Committee on Research (ECOR) support; and has consulting agreements with Boston Scientific and Abbott Vascular. Massachusetts General Hospital has a patent licensing arrangement with Terumo and Canon Corporations. All other authors have reported that they have no relationships relevant to the contents of this paper to disclose. Drs. Verjans, Osborn, and Ughi are joint first authors. Drs. Jaffer and Tearney are joint senior authors.

Manuscript received November 30, 2015; revised manuscript received January 12, 2016, accepted January 14, 2016.

NIRF IMAGING OF ICG-ENHANCED HUMAN CAROTID PLAQUES. Intra-arterial NIRF-OCT and fluorescence reflectance imaging. After surgical resection, the carotid plaque specimen was placed in cold saline for immediate ex vivo intravascular NIRF-OCT. The NIRF-OCT catheter was carefully inserted within the lumen, traversing the common and internal carotid arteries. Two NIRF-OCT pullbacks were performed per sample for reproducibility, followed by macroscopic fluorescence reflectance imaging, as previously described (3,5). In brief, the NIRF-OCT imaging catheter and system acquire simultaneous NIRF and OCT data at a speed of 52 kHz (25.4 frames/s with 2,048 A-lines per image) and pullback velocity of 10 mm/s. OCT images have an axial resolution of ~10 to 15 μm in tissue, a lateral resolution of ~30 μm and signal-to-noise ratio of >110 dB. NIRF images have a lateral resolution of 100 to 200 μm with a signal-to-noise ratio of 51 dB at a concentration of 100 nM ICG. The NIRF-OCT imaging catheter possesses an external diameter of 0.8 mm (2.4-F), similar to the dimensions of existing clinical single-modality OCT catheters. Fluorescence reflectance imaging (Kodak Image-Station 4000, Carestream Health, Rochester, New York) was performed at exposure times of 4 and 64 s for fluorescein isothiocyanate autofluorescence (excitation/emission 470/535 nm) and NIRF (excitation/emission 740/790 nm), respectively.

Microscopic detection of ICG-enhanced human atheroma. After ex vivo imaging, CEA tissue was embedded fresh into optimal cutting temperature media. Next, serial 8-μm cryostat sections were obtained. Fluorescence and brightfield microscopy was performed with an epifluorescence microscope (Nikon Eclipse 90i, Tokyo, Japan). Autofluorescence was detected with a fluorescein isothiocyanate filter (excitation/emission 480/535 nm) and ICG was detected with a near-infrared filter (excitation/emission 775/845 nm) (7).

Matched histological sections corresponding to the NIRF-OCT cross-sectional images were stained with hematoxylin and eosin, Masson trichrome, Oil Red O, Movat Pentachrome, or Carstairs according to the manufacturer's recommendations. CD68 immunostaining was performed on fresh frozen cryostat sections fixed in 1:1 acetone-methanol for 10 min (−20°C), air-dried, and blocked with protein blocking solution for 30 min. Primary monoclonal mouse antihuman antibodies for macrophages (CD68 clone EBM11, 1:200 dilution, Dako North America, Carpinteria, California) were applied overnight in a humidified chamber at 4°C. Sections were then incubated with MACH2-labeled alkaline phosphatase polymer secondary and visualized with Vulcan fast red chromagen (Biocare Medical, Concord, California).

INTRACORONARY NIRF-OCT AND HISTOPATHOLOGY OF ICG-ENHANCED PLAQUES IN SWINE CORONARY ATHEROMA. Please see the Online Appendix for supplemental methods.

RESULTS

As part of the BRIGHT-CEA trial, 5 electively scheduled patients undergoing CEA received ICG intravenously before surgery (0.25 mg/kg up to 25 mg). Three control CEA patients received saline. Surgical resection occurred 99 ± 25 min after ICG injection. No adverse events related to ICG were reported during hospitalization or at 30-day follow-up telephone contact.

INTRAVASCULAR NIRF-OCT DETECTS ICG DEPOSITION IN HUMAN CAROTID PLAQUES. Immediately after surgical resection, freshly isolated carotid plaques underwent ex vivo intra-arterial NIRF-OCT (4), fluorescence reflectance imaging, and correlative histopathology. Distance-corrected, quantitative intravascular NIRF-OCT imaging was performed as before (8). Focal NIRF plaque signal was evident in all 5 ICG patients (**Figures 1 and 2**). ICG NIRF signal was highest in or adjacent to the most stenotic area of the internal carotid artery. Minimally diseased areas yielded scant ICG NIRF signal (**Figure 2**). Plaques from control patients also exhibited little NIRF signal, which is consistent with low near-infrared autofluorescence in tissues (1). Simultaneously acquired coregistered OCT images exhibited bulky plaques with abundant lipid-rich areas.

ICG DEPOSITS BENEATH AREAS OF IMPAIRED ENDOTHELIAL BARRIER FUNCTION. Detailed fluorescence microscopy and histopathological analyses revealed new targeting profiles of ICG in human atherosclerosis. ICG deposited beneath areas of endothelial disruption, including plaques with macrophage and lipid infiltration (**Figure 1**) or frankly disrupted (**Figure 3**) fibrous caps. Directly beneath these areas of endothelial abnormality, ICG was spatially related to macrophage-rich and lipid-rich zones (**Figure 1**, Online Figure 1), extending results from our previous experimental study (5). The human carotid studies also revealed a new target of ICG in plaques: deposition into areas of intraplaque hemorrhage (as detected by Carstairs fibrin stains and Masson trichrome) (**Figure 4**, Online Figures 1A and 1B).

ICG ENABLES INTRAVASCULAR NIRF-OCT IMAGING OF CORONARY ATHEROSCLEROSIS IN VIVO. In the second part of this translational study, we investigated

FIGURE 1 ICG Targets Human Carotid Atherosclerosis In Vivo in Areas of Endothelial Discontinuity, and NIRF Imaging Can Detect ICG Deposition

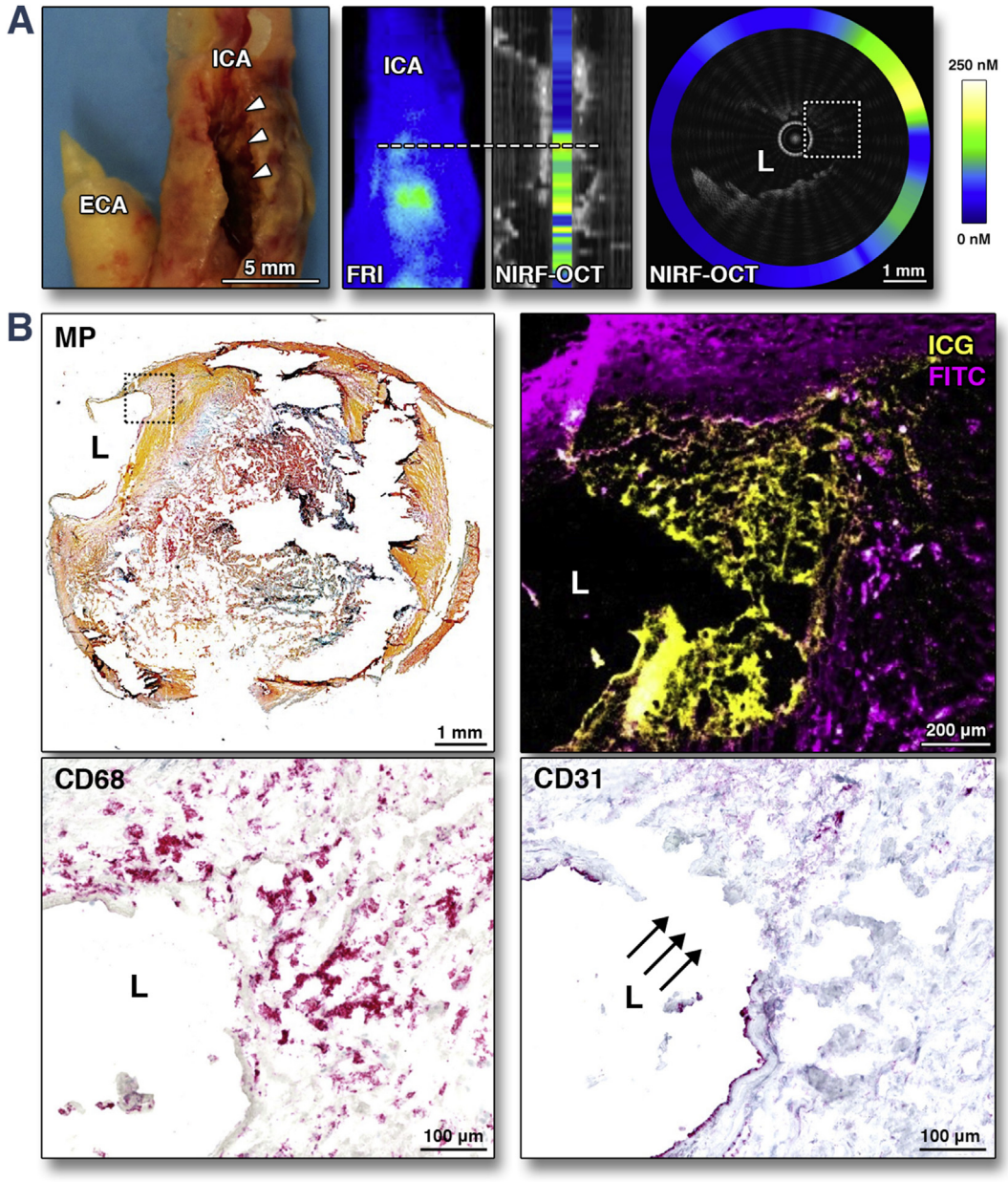

Indocyanine green (ICG) was intravenously injected ~1.5 h before harvest of a representative carotid endarterectomy specimen. **(A)** Photograph and corresponding near-infrared fluorescence reflectance image (FRI), demonstrating similar morphology and corresponding ICG uptake pattern (**light blue** = low ICG signal; **green-yellow** = high ICG signal) at the stenotic region **(white arrowheads)** in the internal carotid artery (ICA). **(Upper row middle right)** The image shows an intravascular near-infrared fluorescence optical coherence tomography (NIRF-OCT) longitudinal fusion image that is anatomically coregistered with the FRI image. The **vertical bar** inside the lumen (L) in this image depicts the average NIRF signal per cross section. **(Upper right)** This image shows a NIRF-OCT cross-sectional fusion image at the area along the **white dashed line** on the FRI and NIRF-OCT longitudinal fusion images. OCT displays decreased signal intensity at the plaque surface, which is consistent with a thinned or absent fibrous cap **(white dotted box)**. In this area of diminished OCT signal, increased NIRF signal is evident, represented by the color-scaled circle. **(B)** Histological analysis of the same area of the cross-sectional image shown in the **right image** of **A**. Movat pentachrome (MP) reveals a complex atherosclerotic plaque with a large necrotic core with lipid and cellular infiltration **(dotted box)**. Higher magnification (10×) fluorescence microscopy of the boxed area reveals ICG NIRF signal adjacent to the lumen, which is distinct from fluorescein isothiocyanate (FITC)-channel autofluorescence. CD68 staining of this same area demonstrates that the ICG NIRF signal **(yellow pseudocolor)** spatially relates to CD68-defined plaque macrophages beneath the area of intimal disruption. The disruption is confirmed by CD31 staining in this same area. ECA = external carotid artery.

FIGURE 2 Additional Representative Ex Vivo NIRF Imaging Examples of 2 Carotid Plaques After ICG Injection, and 2 Control Plaques Without ICG

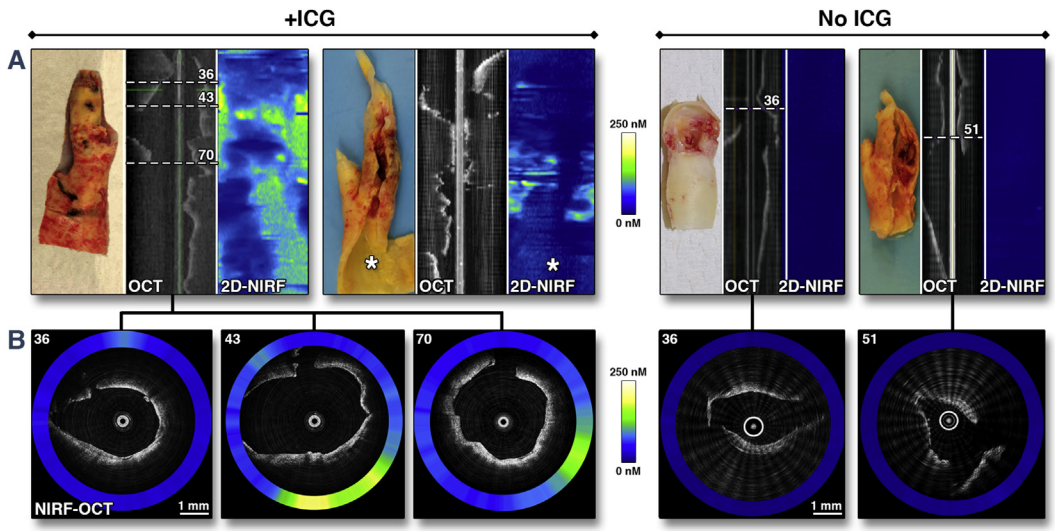

(A) From **left** to **right,** gross photograph, aligned OCT longitudinal image and 2-dimensional (2D) NIRF map (horizontal axis = 0° to 360°, vertical axis = catheter pullback distance), respectively, of 2 plaques from ICG-injected patients (+ICG) and 2 control plaques (no ICG). Pullbacks were performed with the NIRF-OCT catheter positioned within the lumen of the resected carotid artery specimens. **(B)** Representative simultaneously acquired and coregistered NIRF-OCT cross-sectional fusion images from ICG-injected subjects shown on the **left panel** of images in **A**. NIRF-OCT demonstrates areas of elevated ICG signal localization within each internal carotid artery plaque (**left panel** in **B,** axial **white dotted line** slices 36, 43, and 70 in the OCT image in **A**). The **right panels** in **B** show 2 axial NIRF-OCT images from saline-injected control plaques (**white dotted lines** 36 and 51) that reveal minimal near-infrared autofluorescence signal. The quantitative NIRF scale bars shown (0 to 250 nM) apply identically to all NIRF images from **A** and **B**. Abbreviations as in Figure 1.

whether ICG could target intracoronary NIRF plaque imaging in vivo. One of the 4 swine investigated developed coronary atheroma detectable by intravascular ultrasound. This animal received ICG (0.25 mg/kg intravenously). Five hours later, intracoronary NIRF-OCT demonstrated focal NIRF signal in areas of lipid-rich plaque in the left anterior descending artery (**Figure 5**). NIRF microscopy revealed that ICG was spatially related to a deep calcified nodule in this swine model of atherosclerosis.

DISCUSSION

In this first-in-human investigation of targeted ICG NIRF imaging of human atherosclerosis, we found that U.S. Food and Drug Administration-approved ICG deposits in human carotid plaques and is detectable by NIRF imaging; illuminates the plaque feature of impaired endothelial integrity; and, beneath such areas of endothelial compromise, localizes in zones of macrophages, lipid, and notably intraplaque hemorrhage.

Impaired endothelial barrier function promotes atherogenesis by facilitating lipid transport (9), leukocyte transmigration (10), and intraplaque hemorrhage (11). Here we show that ICG-enhanced NIRF imaging provides a novel approach for imaging impaired endothelial integrity, a form of endothelial dysfunction (12,13), in advanced human plaques. ICG did not diffusely illuminate all areas of atherosclerosis (**Figures 1A and 2A**); rather, it deposited adjacent to areas of endothelial compromise with advanced features such as plaque disruption or intraplaque hemorrhage. ICG deposited in regions of overt endothelial disruption (**Figures 1 and 3**) overlying areas of macrophage infiltration (**Figure 1**, Online Figure 1), and areas of intraplaque hemorrhage (**Figure 4**, Online Figure 1). Whereas ICG is a small molecule (molecular weight: 775 kDa), on injection into blood, ICG primarily binds to albumin (14) and secondarily to lipoproteins, as was previously shown directly by size exclusion chromatography (5). Therefore, ICG is anticipated to follow a deposition pattern similar to albumin, which can localize to damaged intimal layers in atheroma and in areas of injured endothelium (15,16). The overall results demonstrate that ICG deposition demarcates plaque areas that harbor a compromised endothelial barrier.

FIGURE 3 ICG Deposits Directly Beneath an Area of Subclinical Carotid Plaque Rupture With Endothelial Discontinuity and Atherothrombosis (Estimated 1 to 2 Weeks Old)

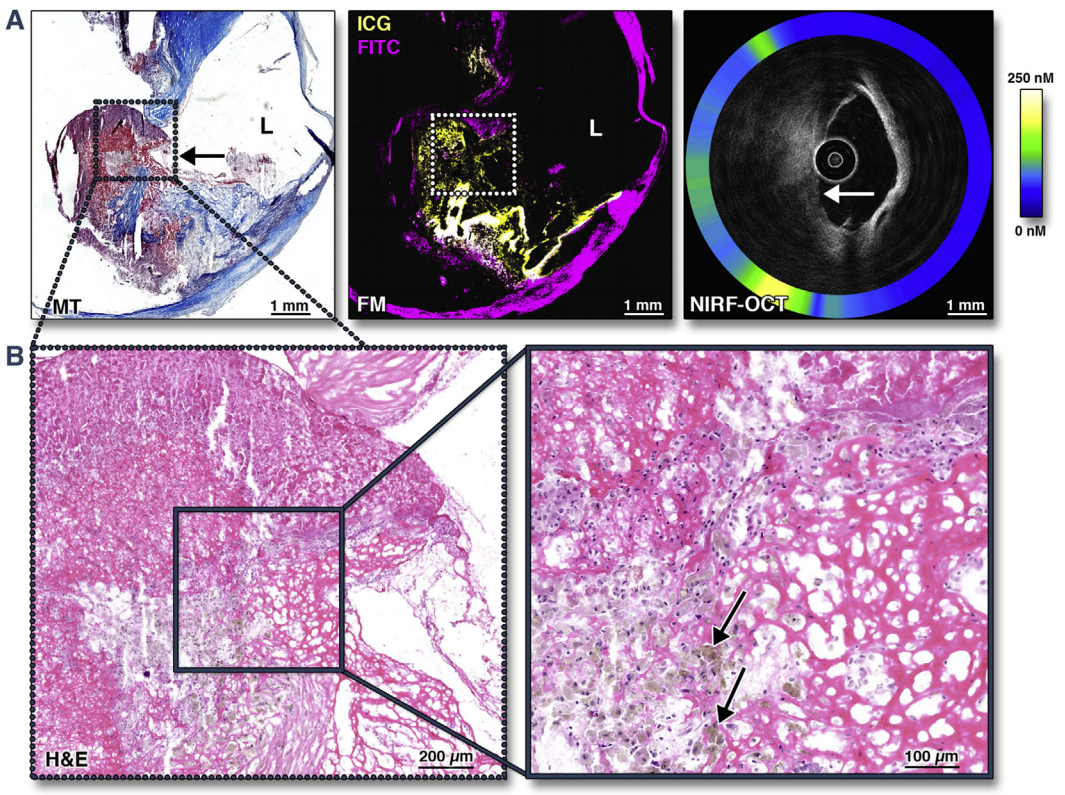

(A) Low-magnification Masson trichrome (MT) and fluorescence microscopy (**purple** = FITC-channel autofluorescence, **yellow** = ICG). The MT stain demonstrates frank plaque rupture (disruption of **blue** collagen fibers, **black arrows**) and protrusion of the necrotic core into the lumen. An adjacent fluorescence microscopy (FM) section **(middle image)** reveals strong ICG colocalization deposition **(yellow)** in the region of plaque rupture. The anatomically coregistered NIRF-OCT fusion image **(right image)** demonstrates high ICG signal by NIRF and plaque surface irregularity by OCT in the regions corresponding to the histological plaque rupture zone (**white arrow;** quantitative NIRF scale bar 0 to 250 nM). **(B)** Low and high magnification H&E staining demonstrated evidence of **brown pigment,** consistent with hemosiderin within macrophages **(arrows)** and areas with fibrin. These features indicate that plaque rupture with atherothrombosis occurred subacutely, rather than acute plaque hemorrhage as a direct consequence of surgery. H&E = hematoxylin and eosin; other abbreviations as in Figure 1.

The ICG targeting pattern observed in this human atherosclerosis study merits discussion in comparison to previous experimental results. In rabbit atherosclerosis, ICG localized to macrophage-rich and lipid-rich atheroma (5,6), and in vitro human studies demonstrated that ICG could label human macrophages and bind acetylated low-density lipoprotein (5). Of note, 1 previous study (5) demonstrated that ICG also deposited in areas of impaired endothelial barrier function, which was highlighted by Evans Blue extravasation into ICG-positive plaques. In the current human study, we found that ICG could bind zones of atheroma governed by endothelial compromise. We postulate that the greater size of human carotid plaques (~10-fold thicker than rabbit atheroma) revealed that ICG has diffusion limits as it interacts with larger atheroma, a finding potentiated by ICG's relatively short blood half-life of 3 to 5 min. Whereas deposition of ICG occurred in certain regions of human plaque macrophages and lipid, binding was not as specific as in the previous rabbit study, suggesting the presence of additional ICG binding targets in human atheroma. To this point, we discovered that ICG could deposit in areas of human intraplaque hemorrhage (fibrin-positive areas in **Figure 4** and Online Figure 1), a new finding compared with those of previous studies of atherosclerotic rabbits, whose lesions do not routinely develop intraplaque hemorrhage. Intraplaque hemorrhage is a high-risk plaque feature that occurs in the setting of plaque neovascularization and can drive plaque progression and adverse clinical events (11,17). Mechanisms

FIGURE 4 ICG Deposits in Areas of IPH in a Human Atheroma

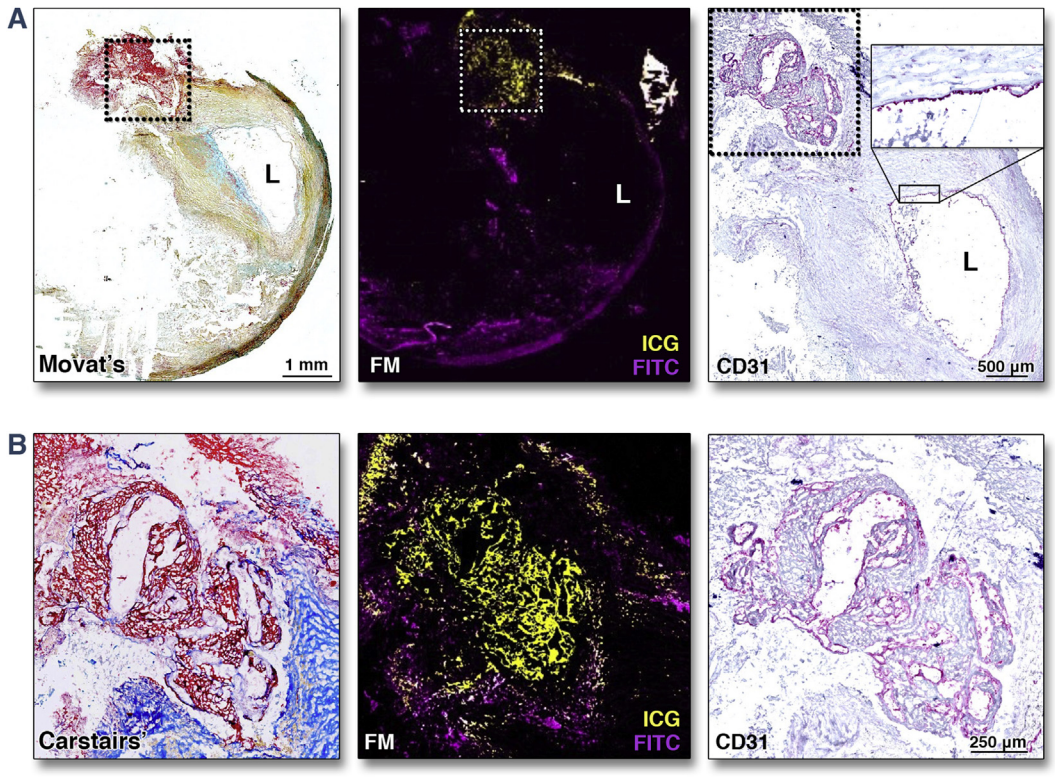

(A) Low magnification Movat pentachrome staining and FM (**purple** = FITC-channel autofluorescence, **yellow** = ICG) reveal strong ICG uptake at a location of plaque hemorrhage beneath the highly stenotic plaque lumen (L), that was clearly demarcated by CD31 (**right top,** high magnification box). **(B)** Higher magnification (5×) FM of the **dashed box** area in **A** demonstrates a large circumscribed zone of ICG-positive signal that colocalizes with intraplaque hemorrhage (IPH) (Carstairs fibrin staining, **red**) and CD31 staining demonstrates that neovessels are present in the area of IPH, offering a potential pathway for ICG extravasation. Abbreviations as in Figures 1 and 3.

underlying the retention of ICG in regions of intraplaque hemorrhage merit further investigation. Finally, imaging of ICG occurred on average 99 min after ICG injection and surgical resection, a longer period than in rabbits where detection of ICG occurred within 20 min after injection. The ability of ICG imaging in human plaques at earlier time points using intravascular NIRF-OCT merits future clinical studies.

Despite the relatively small volume of plaque labeled by ICG, the targeted volume sufficed to enable intravascular NIRF-OCT of human plaques ex vivo and swine coronary plaques in vivo. The detected concentration of the ICG near-infrared fluorophore in human plaques ex vivo and swine plaques in vivo, ranging up to 250 nM, is a similar concentration that permitted in vivo NIRF-OCT imaging of rabbit atherosclerosis (3). The overall study results thus lend support for an intracoronary NIRF imaging trial of ICG for detecting high-risk features of coronary plaques characterized by abnormal endothelial barrier function, a feature that conventional approaches cannot detect in vivo in human coronary plaques. Therefore, ICG NIRF provides additional information beyond OCT by detecting regions with plaque disruption, impaired endothelial integrity, and intraplaque hemorrhage not visualized by OCT. We thus postulate that ICG, through its capacity to detect regions of endothelial compromise, provides additional information that, in principle, can be used to differentiate high-risk from low-risk fibroatheroma. For example, a subset of thin cap fibroatheromas that exhibits ICG NIRF signal might have higher risk of provoking a clinical thrombotic event than a subset of ICG-negative thin cap fibroatheromas. The current study provides a foundation for formal testing of this hypothesis. Translationally, intracoronary NIRF molecular imaging is accelerating into the clinical arena (18,19) and encouragingly, a recent clinical study demonstrates the ability to perform human

FIGURE 5 Intracoronary NIRF-OCT and Histological Assessment of ICG Deposition in Swine Atherosclerosis

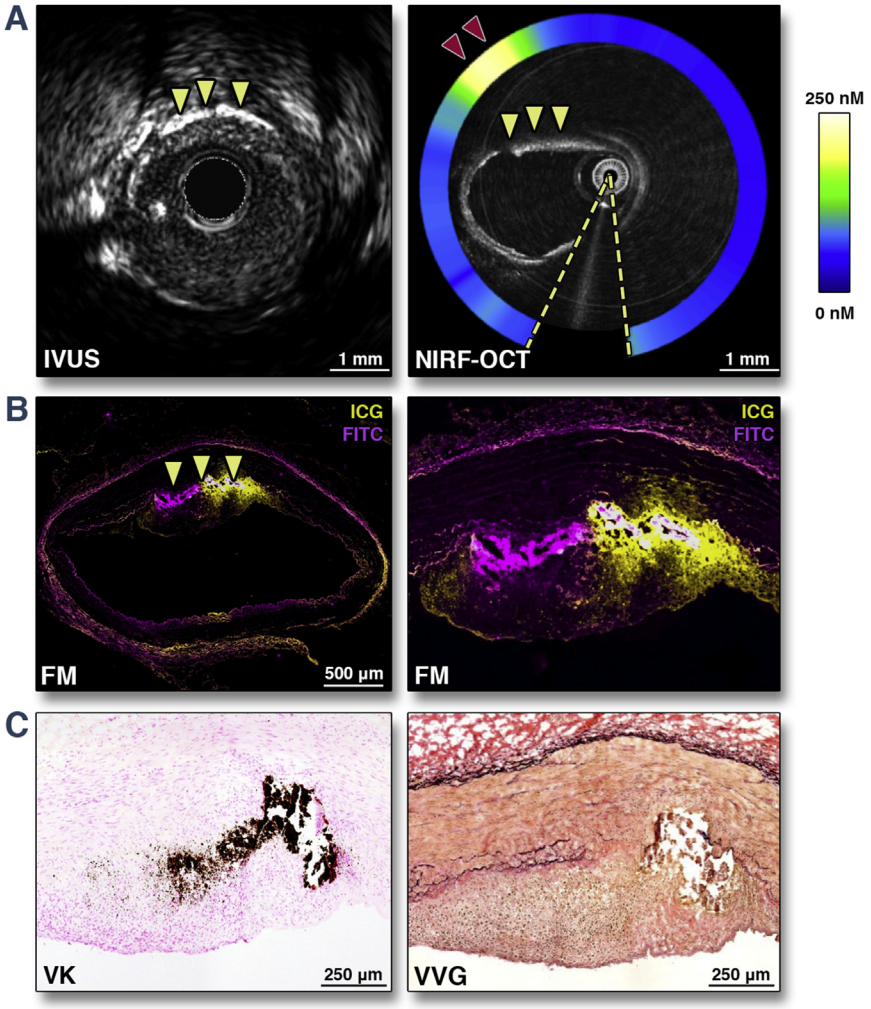

(A) Coregistered intravascular ultrasound (IVUS) and NIRF-OCT cross-sectional fusion images in the left anterior descending artery, with NIRF signal detecting up to 250 nM of ICG (**red arrowheads** denote high ICG NIRF signal, **yellow/white color** at 10 o'clock). Coronary atheroma demonstrates heterogeneous ICG plaque uptake in a lesion with intimal and medial calcification **(yellow arrowheads)**. The plaque morphology and calcified region allowed precise coregistration among IVUS, NIRF-OCT, and histology. Artifact from the intracoronary guidewire (**dashed yellow lines,** NIRF-OCT) was excluded from the NIRF signal ring, OCT catheter dimensions: inner bright circle = 0.5 mm diameter; outer faint circle = 0.8 mm diameter. **(B)** FM (**purple** = FITC-channel autofluorescence, **yellow** = ICG) and histological assessment of the calcified coronary atheroma in **A**. Low and high magnification FM **(second row, left)** shows ICG plaque uptake in the same region of the plaque with calcification **(yellow arrowheads). (C)** von Kossa (VK) calcification stain **(dark brown)** and Verhoeff-Van Gieson (VVG) stain confirm the OCT and IVUS images by demonstrating that the calcium resides within the deep intima at the medial border. Abbreviations as in Figures 1 and 3.

intracoronary NIRF-OCT detection of coronary plaque near-infrared autofluorescence (20). This study provides a foundation for targeted NIRF-OCT molecular imaging in humans in the near future.

STUDY LIMITATIONS. As intracoronary NIRF catheter systems for ICG are not yet clinically available, it remains to be determined whether ICG will be detectable within human coronary arteries of living subjects, and whether ICG detection can enhance risk prediction for subjects with coronary artery disease. These questions are planned to be addressed in future clinical studies.

CONCLUSIONS

ICG enables targeted intravascular NIRF imaging of impaired endothelial integrity in human plaques

and in vivo in swine coronary plaques. Within these areas of impaired endothelial barrier function, ICG deposits in accessible zones of human plaques, including regions containing macrophages, lipid, and intraplaque hemorrhage. Intravascular NIRF imaging of ICG may therefore offer a new approach to assess the pathobiology of human coronary plaques.

ACKNOWLEDGMENTS The authors acknowledge Dr. Mireille Rosenberg, Heather Marino, Luke Stone, and Constance Crittenden, Massachusetts General Hospital Research Study Coordinators, for study assistance; Dr. James Stone and Zakir Siddiquee, Massachusetts General Hospital for assistance with histopathology; Dr. Ahmet Umit Coskun, Brigham and Women's Hospital and Northeastern University, for advice on in vivo swine experiments; Dr. Jenny Zhao, Massachusetts General Hospital, for assistance with histopathology; Dr. Joseph Boyle, Imperial College, for helpful discussions; and Dr. Evangelos Gragoudas, Massachusetts General Hospital, for observation of ICG-based retinal angiography.

REPRINT REQUESTS AND CORRESPONDENCE: Dr. Farouc A. Jaffer or Dr. Guillermo J. Tearney, MGH Cardiovascular Research Center, Simches Research Building, Room 3206, 55 Fruit Street, Boston, Massachusetts 02114. E-mail: fjaffer@mgh.harvard.edu OR gtearney@mgh.harvard.edu.

PERSPECTIVES

COMPETENCY IN MEDICAL KNOWLEDGE: Patients with carotid plaques possessing an impaired plaque endothelial barrier bind ICG, a U.S. Food and Drug Administration–approved injectable NIRF imaging agent. In plaques with an impaired endothelial barrier, ICG deposits in zones of macrophages, lipid, and intraplaque hemorrhage.

TRANSLATIONAL OUTLOOK: Translation of ICG-enhanced intracoronary NIRF imaging and OCT may offer a new approach to the simultaneous assessment of plaque pathobiology and microstructure in clinical subjects presenting to the cardiac catheterization laboratory.

REFERENCES

1. Jaffer FA, Calfon MA, Rosenthal A, et al. Two-dimensional intravascular near-infrared fluorescence molecular imaging of inflammation in atherosclerosis and stent-induced vascular injury. J Am Coll Cardiol 2011;57:2516–26.

2. Mulder WJ, Jaffer FA, Fayad ZA, Nahrendorf M. Imaging and nanomedicine in inflammatory atherosclerosis. Sci Transl Med 2014;6:239sr1.

3. Yoo H, Kim JW, Shishkov M, et al. Intra-arterial catheter for simultaneous microstructural and molecular imaging in vivo. Nat Med 2011;17:1680–4.

4. Hope-Ross M, Yannuzzi LA, Gragoudas ES, et al. Adverse reactions due to indocyanine green. Ophthalmology 1994;101:529–33.

5. Vinegoni C, Botnaru I, Aikawa E, et al. Indocyanine green enables near-infrared fluorescence imaging of lipid-rich, inflamed atherosclerotic plaques. Sci Transl Med 2011;3:84ra45.

6. Lee S, Lee MW, Cho HS, et al. Fully integrated high-speed intravascular optical coherence tomography/near-infrared fluorescence structural/molecular imaging in vivo using a clinically available near-infrared fluorescence-emitting indocyanine green to detect inflamed lipid-rich atheromata in coronary-sized vessels. Circ Cardiovasc Interv 2014;7:560–9.

7. Hara T, Bhayana B, Thompson B, et al. Molecular imaging of fibrin deposition in deep vein thrombosis using fibrin-targeted near-infrared fluorescence. J Am Coll Cardiol Img 2012;5:607–15.

8. Ughi GJ, Verjans J, Fard AM, et al. Dual modality intravascular optical coherence tomography (OCT) and near-infrared fluorescence (NIRF) imaging: a fully automated algorithm for the distance-calibration of NIRF signal intensity for quantitative molecular imaging. Int J Cardiovasc Imaging 2015;31:259–68.

9. Rutledge JC, Curry FR, Lenz JF, Davis PA. Low density lipoprotein transport across a microvascular endothelial barrier after permeability is increased. Circ Res 1990;66:486–95.

10. Rao RM, Yang L, Garcia-Cardena G, Luscinskas FW. Endothelial-dependent mechanisms of leukocyte recruitment to the vascular wall. Circ Res 2007;101:234–47.

11. Kolodgie FD, Gold HK, Burke AP, et al. Intraplaque hemorrhage and progression of coronary atheroma. N Engl J Med 2003;349:2316–25.

12. Hirase T, Node K. Endothelial dysfunction as a cellular mechanism for vascular failure. Am J Physiol Heart Circ Physiol 2012;302:H499–505.

13. Fuster V, Moreno PR, Fayad ZA, Corti R, Badimon JJ. Atherothrombosis and high-risk plaque: part I: evolving concepts. J Am Coll Cardiol 2005;46:937–54.

14. Akorn Pharmaceuticals. Product Sell Sheet—Indocyanine Green. 2008. Available at: http://akorn.com/documents/catalog/sell_sheets/17478-701-02.pdf. Accessed March 5, 2015.

15. Adams CW, Morgan RS, Bayliss OB. The differential entry of [125-I] albumin into mildly and severely atheromatous rabbit aortas. Atherosclerosis 1970;11:119–24.

16. Ramirez CA, Colton CK, Smith KA, Stemerman MB, Lees RS. Transport of 125I-albumin across normal and deendothelialized rabbit thoracic aorta in vivo. Arteriosclerosis 1984;4:283–91.

17. Saam T, Hetterich H, Hoffmann V, et al. Meta-analysis and systematic review of the predictive value of carotid plaque hemorrhage on cerebrovascular events by magnetic resonance imaging. J Am Coll Cardiol 2013;62:1081–91.

18. Osborn EA, Jaffer FA. The advancing clinical impact of molecular imaging in CVD. J Am Coll Cardiol Img 2013;6:1327–41.

19. Jaffer FA, Verjans JW. Molecular imaging of atherosclerosis: clinical state-of-the-art. Heart 2014;100:1469–77.

20. Ughi GJ, Wang H, Gerbaud E, et al. Clinical characterization of coronary atherosclerosis with dual-modality OCT and near-infrared autofluorescence imaging. J Am Coll Cardiol Img 2016 Mar 3 [E-pub ahead of print].

KEY WORDS atherosclerosis, endothelium, indocyanine green, inflammation, intraplaque hemorrhage, intravascular imaging, lipid, molecular imaging, near-infrared fluorescence

APPENDIX For an expanded methods section and a supplemental figure, please see the online version of this article.